



Journal of Applied Sciences

ISSN 1812-5654

science
alert

ANSI*net*
an open access publisher
<http://ansinet.com>

Preparation and Characterization of Polylactic Acid/Polycaprolactone Clay Nanocomposites

Wisam H. Hoidy, Mansor B. Ahmad, Emad A. Jaffar Al-Mulla and Nor Azowa Bt Ibrahim
Department of Chemistry, Faculty of Science,
Universiti Putra Malaysia 43400, Serdang, Selangor, Malaysia

Abstract: Biopolymer nanocomposites, which have attracted much attention due to their biodegradability and biocompatibility, have been prepared by melt blending polylactic acid (PLA)/polycaprolactone (PCL) and two types of organoclay (OMMT) include octadecylamine-montmorillonite (ODA-MMT) and fatty hydroxamic acid- montmorillonite (FHA-MMT). Materials were characterized using X-ray Diffraction (XRD), Fourier transform infrared (FTIR) spectroscopy, thermogravimetric analysis (TGA), elemental analysis and scanning electron microscopy (SEM). Mechanical properties were also investigated for these nanocomposites. The nanocomposites showed increasing mechanical properties and thermal stability. XRD results indicated that the materials formed intercalated nanocomposites. SEM morphology showed that increasing content of OMMT reduces the domain size of phase separated particles. Additionally, a solution casting process has been used to prepare these nanocomposites and characterized to compare these results with above process. These nanocomposites offer potential for diversification and application of biopolymer due to their good properties such as improved thermal and mechanical properties.

Key words: Polylactic acid, polycaprolactone, fatty hydroxamic acid, octadecylamine, nanocomposites, blending

INTRODUCTION

Recently, the plastic industry has very strong influence in different aspects in our every day life. In which most of its uses related in short life time. The after-use valorization grabs the attention of many specialized people in these industries. Some scientists believe that one solution of solving a problem of plastic accumulation for the environment involves the using of biodegradable polymers. In this area or field aliphatic polyesters play a crucial role (Franco *et al.*, 2004).

Essentially Polyesters are polymers by which repeating unit that are bonded via ester linkages, there are many types of esters are present in nature and in enzymes that degrade them. There are series of biodegradable aliphatic polyesters are now produced on a commercial level by several companies that make this kind of industries related directly to the biodegradable plastic. Among them poly (lactic acid) (PLA) and poly (ϵ -caprolactone) (PCL) appear to be the most attractive because of their facile availability and good biodegradability. Both PLA and PCL can be obtained through the petro-chemical route and PLA is now available from renewable resources as well. Therefore, PLA and PCL present a great potential with respect to applications in agriculture and in everyday life as biodegradable packaging material (Tsuji and Ishizaka,

2001). There are many limitations of these biodegradable polymers, because there are the poor thermal and mechanical resistance as well as limitation of gas barriers properties, which include the access to industrialized sectors, for instance packaging that includes the usage of how it would be justified when biodegradable is required (Singh *et al.*, 2003). These obstacles could be controlled by enhancing their thermal and mechanical properties through copolymerization, blending and filling techniques. In fact, the addition of nano-sized fillers would effectively confer multifunctional enabling properties to these polymers.

In the last few decades, more over of nanofillers to polymers has drawn wide attention for the potentiality of these fillers to influence a number of polymer properties; for example, polymer layered silicate nanocomposites, because of the nanometer size of the silicate sheets, exhibit, even at low filler content (1-5 wt.%), markedly improved mechanical, thermal, barrier and flame retardance properties, in comparison to the unfilled matrix and to the more conventional microcomposites (Chow and Lok, 2009; Pluta *et al.*, 2002).

Recently, many authors have reported on the characterization and categories of biodegradable polymer based on nanocomposite, Paul *et al.* (2003) reported on the preparation of PLA/MMT nanocomposites by melt intercalation technique using a MMT modified with

bis-(2-hydroxyethyl) methyl (hydrogenated tallow alkyl) ammonium cations (Paul *et al.*, 2003). The preparation of PLA based nanocomposites with three different kinds of layered silicates via solution intercalation method in N-dimethylacetamide, obtaining the formation of intercalated nanocomposites whatever the clay was carried out by Chang *et al.* (2003). In a recent report, Feijoo *et al.* (2005) prepared biodegradable nanocomposites of amorphous poly(lactic acid) and two different types of organically modified montmorillonite obtaining nanocomposites with stacked intercalated and partially exfoliated layers' morphologies.

Pantoustier *et al.* (2002) used the *in situ* intercalative polymerization method for the preparation of PCL-based nanocomposites. They compared the properties of nanocomposites prepared with both pristine MMT and amino dodecanoic acid modified PLA/MMT and PCL nanocomposites prepared by adding two organically modified montmorillonites and one sepiolite were obtained by melt blending (Fukushima *et al.*, 2009). Di *et al.* (2003) have reported the preparation of PCL layered silicate nanocomposites using a twin-screw extruder. They used two different types of organically modified layered silicates for the preparation of nanocomposites and aimed at determining the dependence of clay dispersion on the processing conditions.

Lee *et al.* (2002) and Paula *et al.* (2005) studied the biodegradability of PLA based nanocomposites in order to study their biodegradability and compost processing. They found an increased biodegradation rate as the nanocomposite samples were completely mineralized in short times. This behavior was generally attributed to the high relative hydrophilicity of the clays, allowing an easier permeability of water into the material thus accelerating the hydrolytic degradation process. The highest hydrophilic character of the filler, the fastest degradation of the polymer (Wang *et al.*, 1998).

In this study, we report the preparation and characterization PLA/PCL-MMT to produce nanocomposites using different organoclays. Octadecylamine ODA and fatty hydroxamic acids FHAs were employed to modify MMT. Characterization of nanocomposites was done by various apparatuses. Both melt blending and solution casting process were used to produce these nanocomposites.

MATERIALS AND METHODS

Materials: Sodium montmorillonite used in this study was obtained from Kunimine Ind. Co. Japan. Hexane was from T.J. Baker, USA (2009). Octadecylamine was from Acros

Organics, USA. Polylactic acid was purchased from Japan. Polycaprolactone was obtained from Solvay Caprolactone, Warrington, England. Hydrochloric acid HCl was from Sigma-Aldrich, Germany.

Synthesis of (FHAs): Palm olein was dissolved in hexane with hydroxylamine hydrochloride by reflux at boiling point of hexane for 10 h using a thermostated round bottom flask equipped with water-cooled condenser and mechanical stirrer. After the reaction had finished (product changed the color to green with copper (II) due to its ability to form complex). The product was dissolved in hot hexane and separated from bottom layer by separating funnel. The hexane phase was cooled in an ice bath for 4 h to obtain FHAs and then filtered and washed by hexane for three times and dried in a vacuum desiccators over phosphorous pentoxide.

The same procedure was used to produce the FHAs from palm stearin and corn oil.

Preparation of organoclay: Organoclay was prepared by cationic exchange process where Na^+ in the montmorillonite was exchanged with alkylammonium ion in an aqueous solution. Designated amount of sodium montmorillonite (Na-MMT) was stirred vigorously in 600 mL of hot distilled water for one hour to form a clay suspension. Subsequently, desired amount of surfactant (octadecylamine) which had been dissolved in 400 mL of hot water and desired amount of concentrated acid hydrochloride (HCl) was added into the clay suspension of (octadecylamine). After stirred vigorously for 1 h at 80°C, the organoclay suspension was filtered and washed with distilled water until no chloride was detected with 1.0 M silver nitrate solution. It was then dried at 60°C for 72 h. The dried organoclay (ODA-MMT) was ground until the particle size was less than 100 μm before the preparation of nanocomposite. A similar procedure was used to prepare FHA-MMT. This organophilic clay was designated as ODA-MMT. The effect of amount of intercalation agent was studied by varying the concentration of the intercalation agent and keeping other parameters constant.

Preparation of PLA/PCL-clay nanocomposites, by solution casting: The required amounts of PLA and PCL were dissolved in chloroform. The PCL solution was then transferred into the PLA solution with a dropper and continuous stirring. After all the PCL solution was transferred into the PLA solution, the resultant mixture was then stirred for 1 h. The required modified clay (ODA-MMT) was then added into the dissolved PLA/PCL in the small portion. The mixture was then

refluxed for 1 h and then ultrasonically stirred using the Ultra Sonic Cathode for 5 min to make sure that the clay fully dispersed in the PLA/PCL solution. FHA-MMT was prepared similarly to ODA-MMT to produce organoclay. The nanocomposite was poured into a Petri dish and left to dry the amount of PLA/PCL and the modified clay used are listed in Table 1.

Preparations of PLA/PCL-clay nanocomposites by melt blending:

The designed amount of PLA/PCL ratio were prepared by an internal mixer (Haake Polydrive), using different conditions (temperature, speed and time) in order to obtain the optimum conditions which were 185°C, 50 rpm and 12 min, respectively. To prepare a sample of the composite, a specific amount of PLA was first melted and mixed thoroughly with appropriate amount of PCL for 2 min. Various amounts of organoclays (1, 2, 3, 4, 5, 6 and 7 php) were incorporated into the blend in the 3 min. The mixture was compress-moulded into sheet of 1 mm thickness sheets under a pressure of 100 kg cm⁻¹ in a standard hot press at 150°C for 15 min and cooled pressed process for 10 min to obtain a good blend film (Vu *et al.*, 2001). The amount of PLA, PCL and the organoclays used are listed in Table 2.

Characterization: The FTIR spectra were recorded on Perkin Elmer FTIR 1650 spectrophotometer at ambient temperature using a KBr disk method. The disk containing 0.0010 g of the sample and 0.3000 g of fine grade KBr was scanned at 16 scans at wavenumber range of 400-4000 cm⁻¹.

Table 1: The amounts of PLA/PCL and modified clay for solution casting

| Sample identity | Weight of PLA (g) | Weight of PCL (g) | Weight of organoclay |
|-----------------|-------------------|-------------------|----------------------|
| 8PLA 2PCL | 4.00 | 1.00 | 0.00 |
| 8PLA 2PCL mod 1 | 3.96 | 0.99 | 0.05 |
| 8PLA 2PCL mod 2 | 3.92 | 0.98 | 0.10 |
| 8PLA 2PCL mod 3 | 3.88 | 0.97 | 0.15 |
| 8PLA 2PCL mod 4 | 3.84 | 0.96 | 0.20 |
| 8PLA 2PCL mod 5 | 3.80 | 0.95 | 0.25 |
| 8PLA 2PCL mod 6 | 3.76 | 0.94 | 0.30 |
| 8PLA 2PCL mod 7 | 3.72 | 0.93 | 0.35 |
| 8PLA 2PCL mod 9 | 3.64 | 0.91 | 0.45 |

Table 2: The amount of PLA/PCL and organoclay for melt blending

| Sample identity | Weight of PLA (g) | Weight of PCL (g) | Weight of organoclay |
|-----------------|-------------------|-------------------|----------------------|
| 8PLA 2PCL | 32.00 | 8.00 | 0.00 |
| 8PLA 2PCL mod 1 | 31.68 | 7.92 | 0.40 |
| 8PLA 2PCL mod 2 | 31.36 | 7.84 | 0.80 |
| 8PLA 2PCL mod 3 | 31.04 | 7.76 | 1.20 |
| 8PLA 2PCL mod 4 | 30.72 | 7.68 | 1.60 |
| 8PLA 2PCL mod 5 | 30.40 | 7.60 | 2.00 |
| 8PLA 2PCL mod 6 | 29.08 | 7.52 | 0.40 |
| 8PLA 2PCL mod 7 | 29.76 | 7.44 | 2.80 |
| 8PLA 2PCL mod 9 | 29.12 | 7.28 | 3.60 |

Elemental analyser (LECO CHNS-932) was used for quantitative analysis of amount of intercalation agent present in the organoclay. A sample of approximately 2 mg of organocly burned at 1000°C under oxygen gaseous flow was used for this test. The sulfamethazine was used as standard.

X-ray Diffraction (XRD) study was carried out using shimadzu XRD 6000 diffractometer with Cu-K α radiation ($\lambda = 0.15406$ nm). The diffractogram was scanned in the ranges from 2-10° at a scan rate of 1° min⁻¹.

TG analysis using Perkin Elmer model TGA 7 Thermogravimetric analyzer was used to measure the weight loss of the samples. The samples were heated from 30-800°C with the heating rate of 10°C min⁻¹ under nitrogen atmosphere at the flow rate of 20 mL min⁻¹.

SEM the fractured surfaces of the nanocomposites were studied using a JEOL attached with Oxford Inca Energy 300 EDXFEL scanning electron microscope operated at 20 to 30 KV. The scanning electron micro photographs were recorded at a magnification of 1000 to 3000X. SEM analysis was carried out to investigate polymer splitting, polymer pull-out, debonding, matrix cracking and polymer matrix adhesion. Samples were dehydrated for 45 min before being coated with gold particle using SEM coating unit Baltec SC030 sputter coater

RESULTS

Elemental analysis: The amount of surfactant being intercalated into the clay galleries was calculated based on elemental analysis of the modified clays. The amounts of atom carbon, nitrogen in the sample clay were analyzed by using elemental analyzer. Na-MMT was found to contain 0.46% carbon and 0.15% nitrogen.. The amounts of C, N in Na-MMT, ODA-MMT and FHA-MMT are given in Table 3. The maximum amount of ODA-MMT and FHA-MMT adsorbed was almost equivalent to the cation exchange capacity of the clay indicating that Na⁺ in clay can be easily replaced by the alkylammonium ion (Table 4).

Table 3: Amounts of C, N in Na-MMT, ODA-MMT and FHA-MMT, respectively

| Element | Amount of element presence in clay (%) | | |
|---------|--|---------|---------|
| | Na-MMT | ODA-MMT | FHA-MMT |
| C | 0.46 | 33.1 | 38.6 |
| N | 0.15 | 2.1 | 2.8 |

Table 4: Amount of surfactants presence in the clay layers

| Organoclay | Amount of intercalatant in the modified clay | |
|------------|--|--|
| | Calculation based onatom C (mmol g ⁻¹) | Calculation based onatom N (mmol g ⁻¹) |
| ODA-MMT | 1.51 | 1.39 |
| FHA-MMT | 1.98 | 1.91 |

Fourier transform infrared (FTIR) spectroscopy: The FTIR spectra of PLA, PCL and PLA/PCL blends are shown in Fig. 1. The peaks located at 2998, 2947 and 1751 cm^{-1} of PLA and 2942, 2867 and 1723 cm^{-1} of PCL were assigned to the stretching vibration of $-\text{CH}_2$ and vibration of $-\text{C}=\text{O}$ bonds, respectively; while in the blend materials these peaks were found in the neutralized regions of 2995, 2944 and 1749 cm^{-1} .

The FTIR spectra of the ODA-MMT, PLA/PCL and PLA/PCL nanocomposites are shown in Fig. 2. The spectrum of PLA/PCL nanocomposites show the peaks at 2997 and 2944 cm^{-1} are due to the C-H stretching. The peak for $\text{C}=\text{O}$ bending observed at 1751 cm^{-1} . The peak for C-O bending is at 1184 cm^{-1} . The peak for Si-O stretching is at 460 cm^{-1} (Tyagi *et al.*, 2006).

The FTIR spectra of the FHA-MMT, PLA/PCL and PLA/PCL nanocomposites are shown in Fig. 3. The spectrum of PLA/PCL nanocomposites shows the peak at 3301 cm^{-1} is due to the N-H amide. The peaks at 2945 and 2890 cm^{-1} are due to the C-H stretching. The peak for $\text{C}=\text{O}$ bending absorbed at 1748 cm^{-1} . The peak for C-O bending is at 1183 cm^{-1} . The peak for Si-O stretching is at 400 cm^{-1} .

Thermogravimetric analysis TGA: Thermogravimetric analysis (TGA) is a quantitative measurement of mass change for a material exposed to a controlled temperature program. It also records the temperature of the weight loss region and the maximum temperature of decomposition. TGA detects single or multiple loss steps from room temperature to 1000°C. This measurement was made to determine the thermal stability of the sample. The sample mass loss due to the volatilization of degraded by-product is monitored as a function of a temperature. Inorganic materials are more thermally stable and resistance compared to the organic material. Thus introduction of inorganic particles would greatly improve the thermal stability of organic materials (Huang and Brittain, 2001).

The decomposition of PLA starts at around 265.38°C. The decomposition is rapid above this temperature and it completes at 380.97°C. A total of 98.41% of weight loss was observed in the decomposition of PLA. The DTG curve of PLA in Fig. 5a shows a single peak at 337.49°C. This decomposition corresponds to the complete dissolution of PLA (Ray and Bousmina, 2005). While the PCL starts to decompose at around 289.94°C and it completes at 433.96°C. The decomposition of PCL shows a higher rate of volatile formation and higher rate of chain scission than that of PLA which shows a single peak of DTG curve at 380.47°C (Wu *et al.*, 2009).

Figure 4c and 5c shows the decomposition of PLA/PCL starts at around 290.14°C and completes at

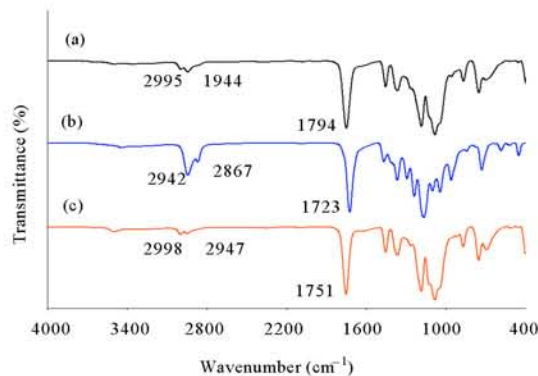


Fig. 1: FTIR spectra of (a) PLA, (b) PCL and (c) PLA/PCL

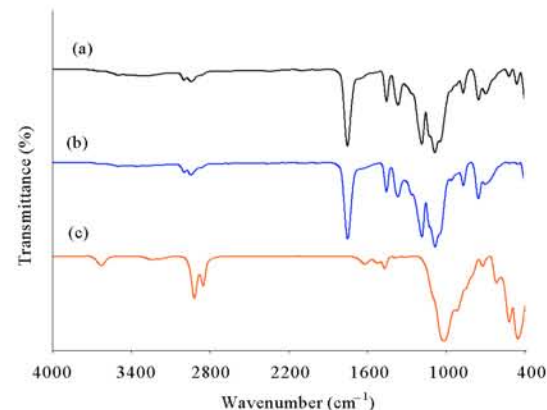


Fig. 2: FTIR spectra of (a) ODA-MMT, (b) PLA/PCL and (c) PLA/PCL-ODA-MMT by melt blending

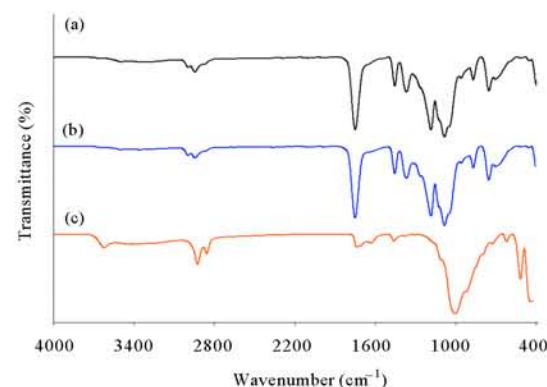


Fig. 3: FTIR spectra of (a) FHA-MMT, (b) PLA/PCL and (c) PLA/PCL-FHA-MMT by melt blending

391.21°C the DTG curve of PLA/PCL nanocomposites in Fig. 5c shows a single peak at 342.15°C. After mixing PLA with PCL, the thermal decomposition of PLA in the blend shifts to the higher temperature region.

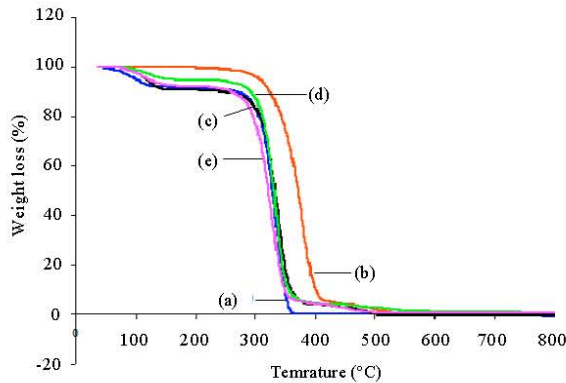


Fig. 4: TGA thermograms of (a) PLA, (b) PCL, (c) PLA/PCL, (d) PLA/PCL-ODA-MMT and (e) PLA/PCL-FHA-MMT

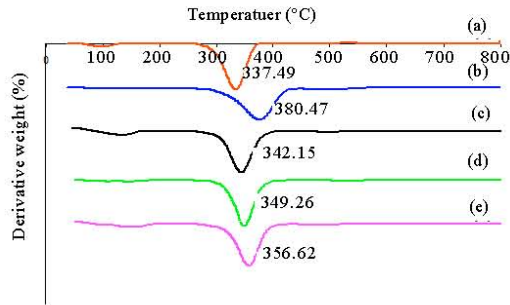


Fig. 5: DTG thermograms of (a) PLA, (b) PCL, (c) PLA/PCL, (d) PLA/PCL-ODA-MMT and (e) PLA/PCL-FHA-MMT

Figure 4d, 5d show the TGA and DTG thermogram of PLA/PCL-ODA-MMT nanocomposites. The degradation temperature of the nanocomposites increase with the adding of ODA-MMT to the PLA/PCL blend, the decomposition of PLA/PCL-ODA-MMT nanocomposites starts at around 299.51°C and completes at 398.51°C the DTG curve of PLA/PCL-ODA-MMT nanocomposites in Fig. 5d shows a single peak at 349.24°C. Figure 4e and 5e show the TGA and DTG thermogram of PLA/PCL-FHA-MMT nanocomposites. The degradation temperature of the nanocomposites increase with the adding of FHA-MMT to the PLA/PCL blend, the decomposition of PLA/PCL-FHA-MMT nanocomposites starts at around 305.21°C and completes at 403.37°C the DTG curve of PLA/PCL-FHA-MMT nanocomposites in Fig. 5e shows a single peak at 354.62°C. The temperature of the main degradation is shifted towards a higher value when OMMT is used compare to the pristine composite.

Tensile strength: The best ratio of tensile strength and modulus properties of PLA/PCL blending in both solution

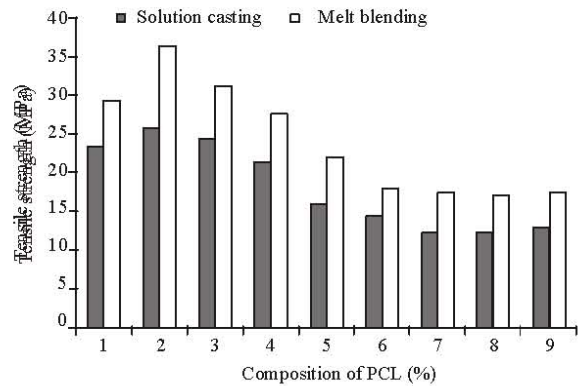


Fig. 6: Effect of adding PCL to PLA on tensile strength by solution casting and melt blending

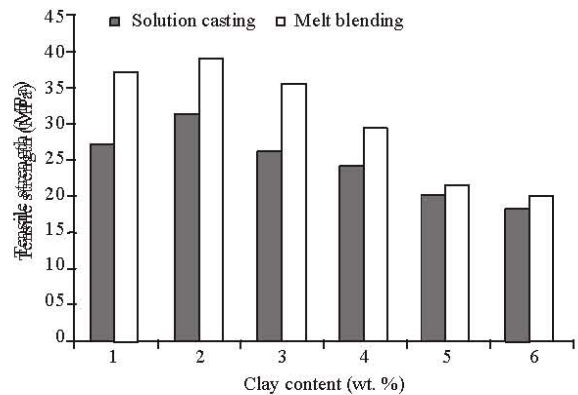


Fig. 7: Tensile strength of 80PLA20PCL with various contents of ODA-MMT prepared by solution casting and melt blending

casting and melt blending was 80/20 (Fig. 6). Therefore, the ratio of 80/20 was used for further experiments.

The tensile properties of polymeric materials can be improved in different degrees if nanocomposites are formed with layered silicates. The tensile strengths of hybrid films with different OMMT contents are shown in Fig. 7, 8. The Fig. 7 and 8 show that low contents of OMMT (2 wt% and 3% for PLA/PCL-ODA-MMT and PLA/PCL-FHA-MMT, respectively). Further increase of the ODA-MMT and FHA-MMT content does not significantly change the tensile strength of the blend.

X-Ray diffraction XRD: The XRD patterns of the PLA/PCL-ODA-MMT and PLA/PCL-FHA-MMT nanocomposites with 1, 2, 3, 4 and 5 php of organoclay loading are given in Fig. 10-13 this results is it agreement with Yu *et al.* (2007). The XRD pattern of ODA-MMT and FHA-MMT show peak 2θ of 3.04 and 2.89 which correspond to the basal spacing 29.47 and 31.02 $^{\circ}\text{A}$,

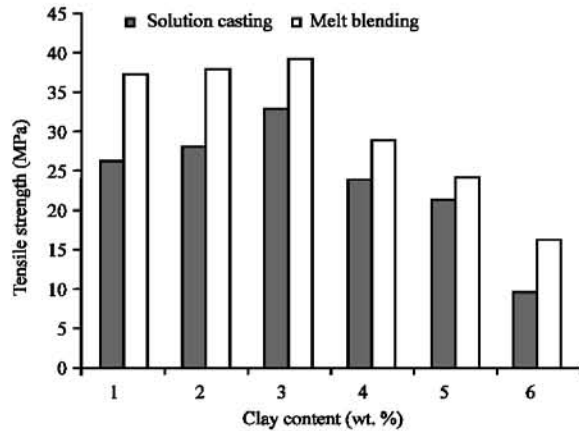


Fig. 8: Tensile strength of 80PLA20PCL with various contents of FHA-MMT prepared by solution casting and melt blending

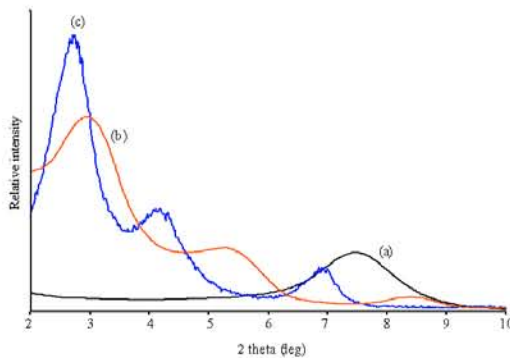


Fig. 9: The XRD patterns of (a) Na-MMT, (b) ODA-MMT and (c) FHA-MMT

respectively (Fig. 9). In solution casting process the XRD of PLA/PCL-ODA-MMT and PLA/PCL-FHA-MMT nanocomposites with 1, 2, 3, 4 and 5 php of ODAMMT and FHA-MMT show shift to lower angles between 2θ of 3.0-2.89 and 2.86-2.70 correspond to the basal spacing between 29.86 -31.02 and 31.35-33.18 °A, respectively (Fig. 10, 11). While in melt blending process the XRD of PLA/PCL-ODA-MMT and PLA/PCL-FHA-MMT nanocomposites with 1, 2, 3, 4 and 5 php of ODAMMT and FHA-MMT show shift to lower angles between 2θ of 2.80-2.61 and 2.82-2.48 correspond to the basal spacing between 32.04-34.61 and 31.79-36.15 °A, respectively (Fig. 12, 13). It is found that PLA/PCL-ODA-MMT nanocomposites with organoclay in solution casting and melt blending loading 2% give the highest basal spacing (31.02 and 34.61°A) while the highest basal spacing of PLA/PCL -FHA-MMT nanocomposites with organoclay in solution casting and melt blending loading 3% was (33.18 and 36.15 °A), respectively.

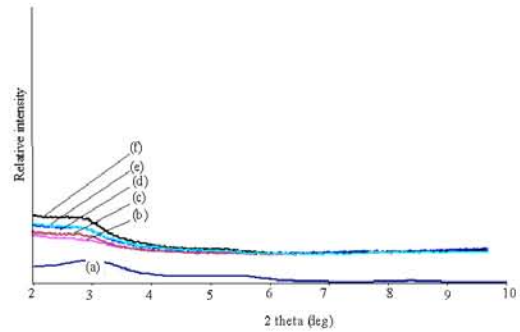


Fig. 10: XRD patterns of (a) ODA-MMT, (b) PLA/PCL/1% ODA-MMT, (c) PLA/PCL/2% ODA-MMT, (d) PLA/PCL/3% ODA-MMT, (e) PLA/PCL/4% ODA-MMT and (f) PLA/PCL 5% ODA-MMT (by solution casting)

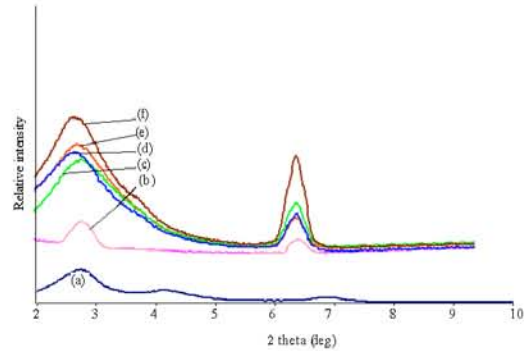


Fig. 11: XRD patterns of (a) FHA-MMT (b) PLA/PCL/1% FHA-MMT, (c) PLA/PCL/2% FHA-MMT, (d) PLA/PCL/3% FHA-MMT, (e) PLA/PCL/4% FHA-MMT and (f) PLA/PCL/5% FHA-MMT (by solution casting)

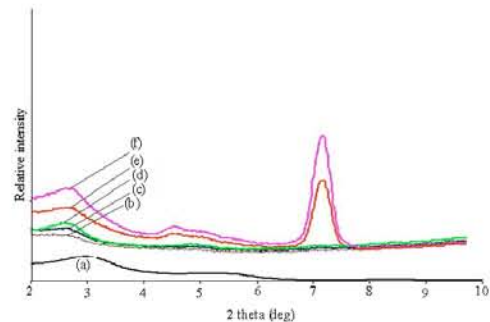


Fig. 12: XRD patterns of (a) ODA-MMT, (b) PLA/PCL/1% ODA-MMT, (c) PLA/PCL/3% ODA-MMT, (d) PLA/PCL/2% ODA-MMT, (e) PLA/PCL/4% ODA-MMT and (f) PLA/PCL/5% ODA-MMT (by melt blending)

Scanning electron microscopy (SEM): Figure 14 shows the SEM images of PLA/PCL blends and PLA/PCL with 2% ODA-MMT and PLA/PCL with 3% FHA-MMT in solution casting and melt blending in the same scale 10 μm . In both of solution casting and melt blending processes, PCL was located inside of the empty voids of the PLA continuous phase. It can be seen that the distribution of PCL in the PLA matrix is homogenous and form single phase morphology (Fig. 14a, b).

Figure 14c, d show PLA/PCL-ODA-MMT and PLA/PCL-FHA-MMT morphology. The incorporation of ODA-MMT and FHA-MMT strongly affect the morphology and thus also the fraction behavior of PLA/PCL nanocomposites which indicate the OMMT flow homogenous in the matrix and form smaller void size.

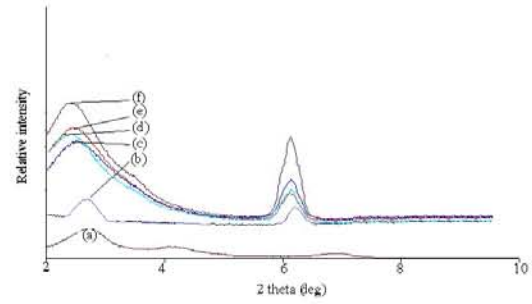


Fig. 13: XRD patterns of (a) FHA-MMT (b) PLA/PCL/1% FHA-MMT, (c) PLA/PCL/2% FHA-MMT, (d) PLA/PCL/3% FHA-MMT, (e) PLA/PCL/4% FHA-MMT and (f) PLA/PCL/5% FHA-MMT (by melt blending)

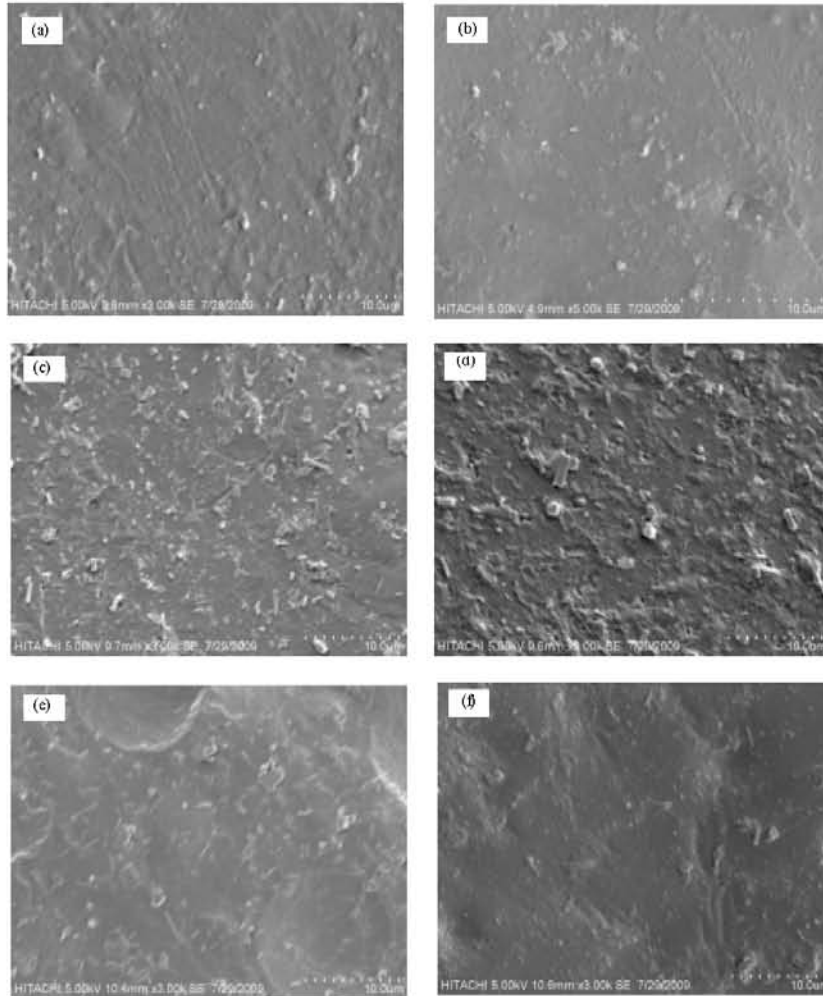
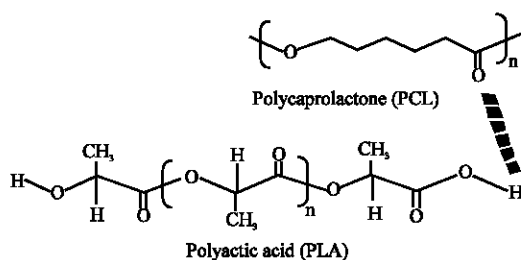


Fig. 14: SEM micrographs of (a) PLA/PCL solution casting, (b) PLA/PCL melt blending, (c) PLA/PCL 2% ODA-MMT melt blending, (d) PLA/PCL 3% FHA-MMT melt blending, (e) PLA/PCL 2% ODA-MMT solution casting and (f) PLA/PCL 3% FHA-MMT solution casting

DISCUSSIONS

The percentage of carbon and nitrogen contents in the organoclay increase after the modification. The calculation is based on either carbon atom or nitrogen atom because if the increase of their content is only due to the presence of the surfactant molecule, the calculation does not based on the hydrogen content as there are possibilities of water molecules trapped between the layers of the Na-MMT.

The FTIR spectra of PLA/PCL blend indicates that there are some molecular interactions between PLA and PCL. The interaction between PLA and PCL may be attributed to the possible hydrogen bonding that occurs between the C = O group in PCL and the small amount of terminal hydroxyl groups in the PLA main chain (Yew *et al.*, 2005). A proposed possible site for interaction between PLA and PCL is shown in Scheme 1. FTIR



Scheme 1: Proposed chemical interactions (intramolecular hydrogen bonding) between PLA and PCL

spectrum of the neat PLA supports this claim which shows peak at 3500 cm^{-1} (hydroxyl group stretching). It was observed that this characteristic peak of PLA has disappeared with the incorporation of PCL.

The FTIR spectra of nanocomposites indicate that both ODA-MMT and FHA-MMT are intercalated with polymers. The above results of FTIR were obtained when the melt blending process was used. It was found that the similar results of FTIR were obtained when solution casting process was used.

The improvement of thermal stability of PLA in the PLA/PCL blend might due to the presence of PCL which acts as toughening filler of PCL and it needs more energy or high temperature to degrade the blend. Chen *et al.* (2003) reported that, the addition of PCL into PLA improves the thermal stability of PLA. It has been reported that the improvement of the stability can be achieved by adding a second polymer (Chen *et al.*, 2003). The increase of thermal stability of PLA was due to the effect of PCL. With the addition of PCL, the molecular chain of PLA was restricted due to reducing its heat sensitivity which would increase thermal stability of PLA (Lee *et al.*, 2002).

It could be observed that organophilic treatment improves the thermal stability of PLA/PCL nanocomposites due to better interaction between PLA/PCL matrix and clay. Incorporated of the ODA-MMT, FHA-MMT in PLA/PCL improves slightly the composites thermal stability. The increase in thermal stability of PLA/PCL/ODA-MMT and PLA/PCL-FHA-MMT nanocomposites may result from the dispersion of the clay and from a strong interaction between the clay platelets and the polymer matrix (Varghese *et al.*, 2003). The above results of TGA and DTG were obtained when the melt blending process was used. It was found that the similar results of TGA and DTG were obtained when solution casting process.

At the higher clay concentration, the organoclay is not homogeneously distributed in the matrix. The agglomeration of the clay causes phase separation (Essawy and El-Nashar, 2004). Both of PLA/PCL-ODA-MMT and PLA/PCL-FHA-MMT nanocomposites prepared by melt blending have higher tensile strength compared with those of solution casting because during polymer intercalation, a relatively large number of solvent molecules have to be absorbed from the host to accommodate the incoming polymer chains especially for higher clay content. Lower tensile strength is obtained for solution casting probably due to insufficient amount of solvent used to accommodate the incoming PLA/PCL chains. In addition, residue of solvent in the final material prepared by solution casting may also causes reduction in tensile strength (Ray and Okamoto, 2003).

Based above result, melt blending process gave higher basal spacing value compare with solution casting process. The above findings indicate that there is intercalation of PLA/PCL into the interlayers of the organoclay prepared by solution casting and melt blending. This means that both methods can be employed to prepared PLA/PCL clay nanocomposites Increase the organoclay content decrease the basal spacing interlayer spacing this because increase the organoclay content will reduce the amount of the polymer intercalated in the galleries of the silicate layers (Vu *et al.*, 2001). These can be also related to the surface accessibility where the closer packing of the silicate layers is more difficult for the polymer chains to penetrate. Based on the above results, intercalated nanocomposites were prepared in this study.

SEM images reveal that the presence of OMMT as a filler enhanced the dispersion and interfacial adhesion of polymer matrix. This observation is agreement with the higher value of tensile strength during tensile test when OMMT is added into composites. A similar morphology was observed when the samples were prepared by solution casting process (Fig. 14e, f).

CONCLUSION

PLA/PCL-OMMT nanocomposites were prepared by both melt blending and solution casting of PLA, PCL and OMMT using ODA and FHA as modifiers of clay. X-ray diffraction (XRD) shows that both methods could be used to synthesize PLA/PCL clay nanocomposites. The silicate layers of the clay were intercalated distributed in the matrix. The addition of OMMT to the PLA/PCL blend significantly improved the tensile properties of nanocomposites. The highest values were obtained when the OMMT content was about 3% (FHA-MMT) and 2% (ODA-MMT). Further amount of organoclays could cause brittleness of nanocomposites. FTIR results indicate that both ODA-MMT and FHA-MMT are intercalated with polymer. On other hand, layered silicate explicitly improved the thermal stability of PLA/PCL blend. SEM images show the incorporation of OMMT strongly affects the morphology which indicate the OMMT flow homogenous in the matrix and form smaller void size. Both PLA/PCL-ODA-MMT and PLA/PCL-FHA-MMT prepared by melt blending gave higher tensile strength and basal spacing compare with those of solution casting. The similar results of FTIR and TGA were obtained in both methods.

REFERENCES

- Chang, J.H., Y.U. An and G.S. Sur, 2003. Synthesis of biodegradable polycaprolactone/montmorillonite nanocomposites by direct in-situ polymerization catalyzed by exchanged clay. *J. Polym. Sci.*, 41: 94-99.
- Chen, C.C., J.Y. Chueh, H. Tseng, H.M. Huang and S.Y. Lee, 2003. Preparation and characterization of biodegradable PLA polymeric blends. *Biomaterials*, 24: 1167-1173.
- Chow, W.S. and S.K. Lok, 2009. Thermal properties of poly(lactic acid)/organo-montmorillonite nanocomposites. *J. Thermal. Anal. Cal.*, 95: 627-632.
- Di, Y., S. Iannace, E.D. Maio and L. Nicolais, 2003. Reactively modified poly(lactic acid): Properties and foam processing. *J. Polym. Sci.*, 41: 670-675.
- Essawy, H. and D. El-Nashar, 2004. The use of montmorillonite as a reinforcing and compatibilizing filler for NBR/SBR rubber blend. *Polym. Test.*, 23: 803-807.
- Feijoo, J.L., L. Cabedo, E. Giménez, J.M. Lagaron and J.J. Saura, 2005. Development of amorphous PLA-montmorillonite nanocomposites. *J. Mater. Sci.*, 40: 1785-1788.
- Franco, C.R., V.P. Cyras, J.P. Busalmen, R.A. Ruseckaite and A. Vázquez, 2004. Degradation of polycaprolactone/starch blends and composites with sisal fibre. *Polym. Degrad. Stab.*, 86: 95-103.
- Fukushima, K., D. Tabuani and G. Camino, 2009. Nanocomposites of PLA and PCL based on montmorillonite and sepiolite. *Mater. Sci. Eng. C.*, 29: 1433-1441.
- Huang, X. and W.J. Brittain, 2001. Synthesis and Characterization of PMMA nanocomposite by suspension and emulsion polymerization. *Macromolecules*, 34: 3255-3260.
- Lee, S.R., H.M. Park, H. Lim, T. Kang, X. Li and W.J. Cho, 2002. Microstructure, tensile properties and biodegradability of aliphatic polyester/clay nanocomposites. *Polymer*, 43: 2495-2500.
- Pantoustier, N., B. Lepoittevin, M. Alexandre, P. Dubois, D. Kubies, C. Calberg and R. Jérôme, 2002. Biodegradable polyester layered silicate nanocomposites based on poly (ϵ -caprolactone). *Polym. Eng. Sci.*, 42: 1928-1937.
- Paul, M.A., M. Alexandre, P. Degée, C. Henrist, A. Rulmont and P. Dubois, 2003. New nanocomposite materials based on plasticized poly(L-lactide) and organo-modified montmorillonites thermal and morphological study. *Polymer*, 44: 443-450.
- Paula, M.A., C. Delcourta, M. Alexandria, P. Degée, F. Monteverdeb and P. Dubois, 2005. Polylactide/montmorillonite nanocomposites study of the hydrolytic degradation. *Polym. Degrad. Stab.*, 87: 535-542.
- Pluta, M., A. Galeski, M. Alexandre, M.A. Paul and P. Dubois, 2002. Poly (lactide)/montmorillonite nano- and microcomposites prepared by melt blending. Structure and some physical properties. *J. Appl. Polym. Sci.*, 86: 1497-1506.
- Ray, S.S. and M. Okamoto, 2003. Polymer/layer silicate nanocomposites: A review from preparation to processing. *Prog. Polym. Sci.*, 28: 1539-1641.
- Ray, S.S. and M. Bousmina, 2005. Biodegradable polymers and their layered silicate nanocomposites in greening the 21st century materials world. *Prog. Mater. Sci.*, 50: 962-1079.
- Singh, R.P., J.K. Pandey, D. Rutot, P. Degée and P. Dubois, 2003. Biodegradation of poly (ϵ -caprolactone)/starch blends and composites in composting and culture environments: The effect of compatibilization on the inherent biodegradability of the host polymer. *Carbohydr. Res.*, 338: 1759-1769.
- Tsuji, H. and T. Ishizaka, 2001. Blends of aliphatic polyesters. VI. Lipase-catalyzed hydrolysis and visualized phase structure of biodegradable blends from poly(ϵ -caprolactone) and poly (L-lactide). *Int. J. Biol. Macro.*, 29: 83-89.

- Tyagi, B., D.C. Chintan and V.J. Raksh, 2006. Determination of structural modification in acid activated montmorillonite clay by FT-IR spectroscopy. *Spectrochimica Acta*, 64: 273-278.
- Varghese, S., J.K. Kocsis and K.G. Gatos, 2003. Melt-compounded epoxidized natural rubber/layered silicate nanocomposites: Structure-properties relationships. *Polymer*, 44: 3977-3983.
- Vu, Y.T., J.E. Mark, H. Pham and M. Engelhardt, 2001. Clay nanolayer reinforcement of cis-1,4-polyisoprene and epoxidized natural rubber. *J. Appl. Polym. Sci.*, 82: 1391-1403.
- Wang, L., W. Ma, R.A. Gross and S.P. McCarthy, 1998. Reactive compatibilization of biodegradable blends of poly (lactic acid) and poly (ϵ -caprolactone). *Polym. Degrad. Stab.*, 59: 161-168.
- Wu, T., T. Xie and G. Yang, 2009. Preparation and characterization of poly(ϵ -caprolactone)/Na⁺-MMT nanocomposites. *Appl. Clay. Sci.*, 45: 105-110.
- Yew, G.H., A.M. Yusof, Z.A. Ishak and U.S. Ishiku, 2005. Water absorption and enzymatic degradation of poly(lactic acid)/rice starch composites. *Polym. Degrad. Stab.*, 90: 488-500.
- Yu, Z., J. Yin, S. Yan, Y. Xie, J. Ma and X. Chen, 2007. Biodegradable poly(L-lactide)/poly(ϵ -caprolactone)-modified montmorillonite nanocomposites: Preparation and characterization. *Polymer*, 48: 6439-6447.